

Proprioceptive Guidance of Saccades in Eye–Hand Coordination

L. Ren,^{1,2,5} A. Z. Khan,^{1,3,5} G. Blohm,^{1,2,5} D.Y.P. Henriques,^{1,2,5} L. E. Sergio,^{1,2,5} and J. D. Crawford^{1,2,3,4,5}

¹Centre for Vision Research and ²Departments of Kinesiology and Health Science, ³Psychology, and ⁴Biology, York University, Toronto; and ⁵ Canadian Institutes of Health Research Group for Action and Perception, Ontario, Canada

Submitted 26 September 2005; accepted in final form 12 May 2006

L. Ren, A. Z. Khan, G. Blohm, D.Y.P. Henriques, L. E. Sergio, and J. D. Crawford. Proprioceptive guidance of saccades in eye–hand coordination. *J Neurophysiol* 96: 1464–1477, 2006. First published May 17, 2006; doi:10.1152/jn.01012.2005. The saccade generator updates memorized target representations for saccades during eye and head movements. Here, we tested if proprioceptive feedback from the arm can also update handheld object locations for saccades, and what intrinsic coordinate system(s) is used in this transformation. We measured radial saccades beginning from a central light-emitting diode to 16 target locations arranged peripherally in eight directions and two eccentricities on a horizontal plane in front of subjects. Target locations were either indicated 1) by a visual flash, 2) by the subject actively moving the handheld central target to a peripheral location, 3) by the experimenter passively moving the subject's hand, or 4) through a combination of the above proprioceptive and visual stimuli. Saccade direction was relatively accurate, but subjects showed task-dependent systematic overshoots and variable errors in radial amplitude. Visually guided saccades showed the smallest overshoot, followed by saccades guided by both vision and proprioception, whereas proprioceptively guided saccades showed the largest overshoot. In most tasks, the overall distribution of saccade endpoints was shifted and expanded in a gaze- or head-centered cardinal coordinate system. However, the active proprioception task produced a tilted pattern of errors, apparently weighted toward a limb-centered coordinate system. This suggests the saccade generator receives an efference copy of the arm movement command but fails to compensate for the arm's inertia-related directional anisotropy. Thus the saccade system is able to transform hand-centered somatosensory signals into oculomotor coordinates and combine somatosensory signals with visual inputs, but it seems to have a poorly calibrated internal model of limb properties.

INTRODUCTION

Human behavior consists largely of a succession of actions that require eye–hand coordination. Saccade target locations can be derived from a variety of sensory inputs, such as visual, auditory, and somatosensory information (Bridgeman 1995; Deubel et al. 1998; Pouget et al. 2002), which provide the brain with moment-to-moment information about the location and motion of external targets. Because these internal representations seem to be mainly stored in egocentric coordinates, they must also be updated when the body itself moves (Helmholtz 1962; Stark and Bridgeman 1983). For example, it is well known that gaze-centered representations of remembered target locations for subsequent saccades are updated constantly during eye movements (Colby et al. 1995; Duhamel et al. 1992; Gottlieb et al. 1998; Khan et al. 2005; Medendorp et al. 2003). However, this is not the only situation where the target esti-

mate within the oculomotor system needs to be updated because of self-motion. For example, during manual manipulation of an object, our own hand movements often displace the target with respect to the eye. Currently, it is not known if, or how accurately, humans can use limb proprioception to internally update oculomotor representations in this situation.

Gaze behavior is closely intertwined with hand movements (Abrams et al. 1990; Helsen et al. 2000; Neggers and Bekkering 2000, 2001), but it can be temporarily dissociated from handheld objects to gather information elsewhere during the manipulation of multiple objects, for example in construction tasks or tool use (Johansson et al. 2001). Several studies have suggested that the kinematics of saccades associated with simultaneous movements of the hand is different from those when the eyes move alone (Synder et al. 2002; Van Donkelaar et al. 2004). Moreover, two recent studies indicated that perturbations of limb movements are incorporated into the internal models for saccade generation (Nanayakkara and Shadmehr 2003; Scheidt et al. 2005). However, the spatial accuracy and neural substrates of these feedback signals are unknown.

Cognition is also involved in manually guided saccades: the subject must know that the target is held in the hand and moves along with the hand (Flanagan and Johansson 2003; Johansson et al. 2001; Nanayakkara and Shadmehr 2003; Scheidt et al. 2005). When this information is unambiguous and the position of body and head is stationary, errors associated with saccades to handheld targets might result from two sources: baseline errors associated with the oculomotor system itself and errors specific to the transformation of somatosensory signals of the limb into oculomotor coordinates.

Saccade accuracy to visual and remembered visual targets has been measured in many studies (Henriques and Crawford 2001). With the exception of initial eye position effects, saccade errors are generally small (Henriques and Crawford 2001; White et al. 1994). However, saccades based on somatosensory input from the limbs would depend on a more complex set of transformations and thus might be expected to show a more complex set of errors (Groh and Sparks 1996; Neggers and Bekkering 1999). To transform somatosensory input into oculomotor coordinates, it has been suggested that the system has to have knowledge of the location of the target in the hand relative to the direction of gaze (Andersen and Buneo 2002; Batista et al. 1999; Buneo et al. 2002). This calculation in turn requires a series of reference frame transformations, which depend on knowledge of relative finger, hand, arm, head, and eye configurations, potentially derived from both proprioceptive and efference copy signals (Blakemore et al. 1998; Leube

Address for reprint requests and other correspondence: J. D. Crawford, Rm. 0003F, Computer Science and Engineering Bldg., Ctr. for Vision Research, 4700 Keele St., York University, Toronto, Ontario M3J 1P3, Canada (E-mail: jdc@yorku.ca).

The costs of publication of this article were defrayed in part by the payment of page charges. The article must therefore be hereby marked "advertisement" in accordance with 18 U.S.C. Section 1734 solely to indicate this fact.

et al. 2003; Lewis et al. 1998; Nanayakkara and Shadmehr 2003; Nelson 1996).

Given the above transformations, efference copies of limb commands could potentially provide an accurate measure of limb movements and on-line limb locations, if the system possesses an accurate model of limb biomechanics in the efference feedback loop (Ariff et al. 2002; Nanayakkara and Shadmehr 2003). Hogan (1985) has shown that the inertial resistance (a component of limb biomechanics) for hand movements is not uniform, but varies depending on the direction of hand movement. According to his two-segment model, initial inertial resistance varies with initial hand position and, in the horizontal plane, the maximum inertia of the arm aligns approximately along the extension–flexion axis (Fig. 1A), whereas the direction of minimum inertia aligns approximately along the adduction–abduction axis.

Flanagan and Lolley (2001) showed that the inertial anisotropy of the arm was accurately predicted during movement planning. These findings have been expanded to three-dimensional (3-D) arm positions (Sabes et al. 1998; Soechting et al. 1995). These studies show that a model of the inertial properties of the arm is incorporated into the planning of hand trajectories during reaching and pointing movements. Specifically, because the “power” of required neuromuscular activation depends on the direction of movement, this directional anisotropy must be incorporated into the motor command (Scott et al. 1997; Sergio et al. 2005), and an internal model of limb inertia is also required when efferent copies of the motor outflow are used to estimate the size and direction of the movement. Interestingly, the smooth pursuit system (Vercher et al. 2003) seems to make use of this internal model of limb

inertia (when pursuing a self-generated hand movement), but this has yet to be tested for the saccade generator.

In this study, we hypothesized that spatial representations of handheld targets can be updated by the saccade generator using limb proprioceptive signals and/or efference copies of hand movements. We also hypothesized that saccades show their largest systematic and variable errors in amplitude rather than direction, as shown previously for visually guided saccades (Klier and Crawford 1998; Niemeier et al. 2003; Vindras et al. 2005). However, here this pattern of amplitude errors could take several forms, depending on their source (Fig. 1, B–D). If the amplitude errors are independent of direction (Fig. 1B), this would provide little information about the source of the errors. If there are errors of gain or bias in the spatial coordinates associated with saccades, patterns like those depicted in Fig. 1C might be expected, i.e., shifts or distortions along one or both cardinal axes. Because the oblique movement directions in our experiment coincided with forearm posture in our experiment, extension–flexion and adduction–abduction will form two coordinate axes with different levels of limb inertia. If the saccade generator uses an efference copy of these movements from the limb system but fails to compensate for the inertial anisotropy, shifts or gain distortions will be expected along the oblique coordinates during active hand movement (Fig. 1D).

METHODS

Subjects

Six healthy volunteers (3 males and 3 females) were recruited in this study, whose ages ranged from 22 to 44 yr (mean = 29). All subjects were healthy, with normal or corrected to normal vision. Subjects were naive to the purpose of the experiment and signed informed consent forms for their participation in this study, which was approved by the York University Human Participants Review Subcommittee.

Equipment

Subjects sat in a dark room at the center of a 2-m magnetic search-coil system, with their head immobilized and tilted 45° downward through the use of a personalized dental impression bar (Fig. 2A). Subjects were directed to look down at a horizontal target board that was indented with linear grooves to guide arm movements. The center of the board was aligned to the subjects' midline, at a vertical distance of 30 cm and a horizontal distance of 20 cm from the center of the two eyes. The subject's right hand rested on a hand plate (5 × 10 × 1 cm) with a spring-loaded guide pin placed underneath to slide smoothly along the grooves of the target board. Subjects learned to recognize the central position when the guide-pin slid over a deep indentation at the center of the board. Four grooves were carved along the four perpendicular cardinal x-y-axes, with removable stoppers on each side at 5 and 10 cm from the central indentation. The target board could be rotated by 45° to realign the grooves with the oblique axes, therefore providing 16 peripheral positions in total (Fig. 2A). In addition, a dowel projecting 2 cm upward from the hand plate was held between the subject's right thumb and index finger. A green LED attached to the top of the dowel served as the central target and the peripheral visual cue in the proprioceptive + visual tasks (Fig. 2A). For the visual controls, a set of LEDs were mounted on the target board at exactly the same positions as the dowel/LED in the proprioceptive and proprioceptive + visual tasks.

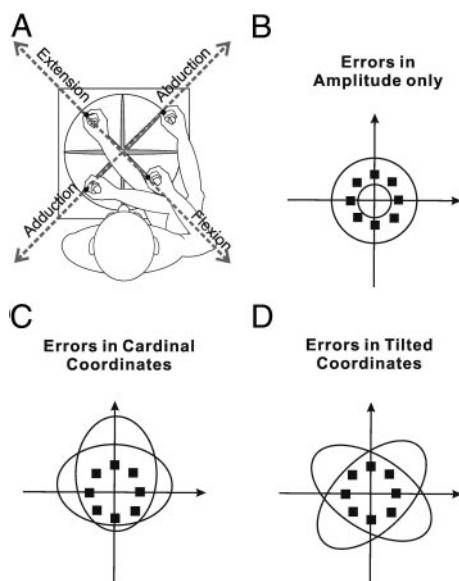


FIG. 1. Potential error patterns for saccades in table coordinates. A: experimental setup. Subjects' arms were positioned so that oblique movement direction aligned with a limb-based coordinate system (extension–flexion vs. abduction–adduction: \leftrightarrow). B–D: possible patterns of saccade errors in table coordinates when a saccade is guided by vision and/or proprioception. Black squares, target locations; empty circles and ellipses, potential error patterns. B: saccade errors in amplitude only with no overall bias (shift). C: saccade errors with amplitude depending on direction in cardinal coordinates, plus an overall bias relative to center position or body. D: error caused by greater saccade amplitude effects either along extension–flexion or abduction–adduction axes of limb coordinates (as shown in A) would lead to tilted elliptical patterns.

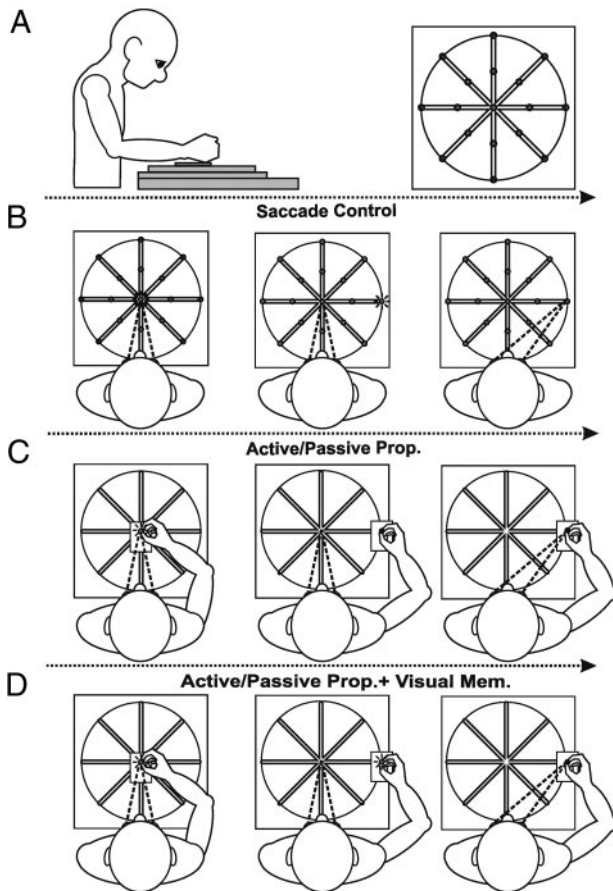


FIG. 2. Experimental setup and paradigms. *A*: *left*: subjects sat in a dark room in front of a horizontal table, with the head fixed (using a bite-bar) at a 45° downward orientation toward the table. Subjects held a short dowel topped by an LED between the right index finger and thumb, with the hand resting on a plate that could slide on a grooved board. *Right*: 16 radial targets (○) viewed from above the table (8 directions, 5 and 10 cm from the center, at visual angles 7 and 13° relative to the center). *B*: visual control paradigms. *Left*: subjects first fixated on illuminated center LED. *Middle*: peripheral LED flashed when center LED disappeared. *Right*: subjects made a saccade to peripheral target with no memory delay [visual saccade (VS)] or after a memory delay [memory saccade (MS)]. Dashed lines are binocular gaze lines. *C*: active/passive proprioception tasks. *Left*: subjects viewed handheld flashed LED at center position. *Middle*: when center target was extinguished, either a computer voice command instructed subjects to move the hand to 1 of the peripheral positions [active proprioception (AP) task] or the hand was passively moved to that location by the experimenter moving the hand plate [passive proprioception (PP) task]. *Right*: auditory beep signaled subject to saccade toward perceived location of nonilluminated LED between their fingers. *D*: active/passive hand movements with additional visual cues. Hand and eye movements were the same as in Fig. 1C with the exception that the LED flashed briefly at final dowel position before subjects made a saccade (AP + VM/PP + VM tasks).

Eye movements were measured using a two-dimensional (2-D) search coil as described previously (Henriques et al. 1998). A scleral 2-D coil (Skalar, Delft, Netherlands) was inserted into the right eye of the subject. The movements of the target and right hand were recorded using an Optotrak 3020 digitizing and motion analysis system (Northern Digital, Waterloo, Ontario, Canada) with infrared emitting diode markers attached to the target and fingertips of index finger and thumb of the right hand. An additional marker was placed at the right temple. Two Optotrak position sensors placed to the left and right of the subject enabled us to record the positions of all markers. Data were sampled from both the Optotrak and search coils at a frequency of 100 Hz and saved on a personal computer for off-line analysis.

Experimental paradigms

In each of the following paradigms, five trials were made to each of the 16 peripheral target locations in computer-randomized order.

PARADIGM 1: VISUAL SACCADE. Subjects began by looking at the central LED that was illuminated for 500 ms and were instructed to maintain fixation at this position in the dark for another 500 ms until a peripheral LED flashed for 100 ms (Figs. 2B and 3A). Subjects were directed to saccade immediately toward the peripheral LED and return fixation back to the center position to await the next trial. Each trial lasted 2,500 ms.

PARADIGM 2: MEMORY SACCADE. This task was similar to paradigm 1 except that subjects were required to continue fixating the center for 900 ms after the peripheral target was flashed and extinguished (Figs. 2B and 3B). At the end of this delay interval, a spatially irrelevant auditory beep signaled subjects to saccade to the remembered location of the peripheral target. After another 700 ms, a second beep signaled subjects to return their gaze to the center and wait for the next trial. The complete time span of this trial was 3,000 ms.

PARADIGM 3: ACTIVE PROPRICEPTION. Here, the handheld central LED was flashed for 500 ms, and a computer-generated voice command instructed the subject to slide the hand plate (as fast as possible) in one of the four cardinal or oblique directions to the end-stopper (Figs. 2C and 3C). The first four cardinal directions were tested in one block, and then the grooved board was rotated horizontally by 45° and the four diagonal directions were tested in a second block. Within each of these two blocks, we measured a subblock that contained short-amplitude movements and another subblock that contained long-amplitude movements. The order of these blocks and subblocks

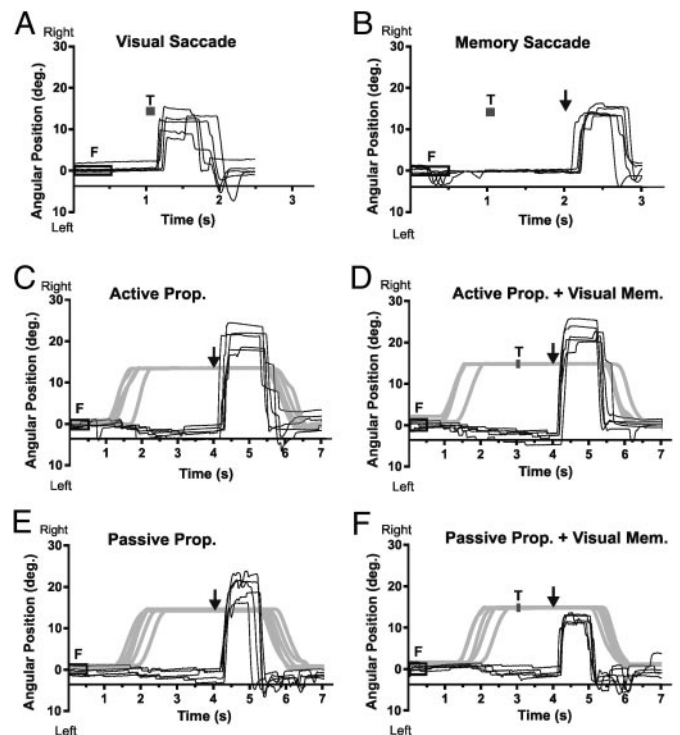


FIG. 3. Sample data from a typical subject: horizontal trajectories of the eye and hand toward the far-right target location. For each of the 6 paradigms, 5 saccades (black traces) are plotted in oculomotor coordinates as a function of time. *A*: VS paradigm. *B*: MS paradigm. *C*: AP paradigm. *D*: AP + VM. *E*: PP paradigm. *F*: PP + VM. □, location and duration of central fixation (F) light; ■, location and duration of saccade target (T) light (13° rightward target here); ↓, beep cue for beginning of saccade; black lines, eye movement trajectories; gray lines, hand movement trajectories.

was counterbalanced equally across subjects. During hand motion, subjects were required to maintain fixation at the center of the board. An auditory beep signaled subjects to saccade toward and fixate the perceived location of the handheld target (specifically, the top of the dowel where the LED was located) 3,500 ms after the central fixation LED was extinguished. One thousand milliseconds later, a second beep signaled subjects to return gaze and hand position back to the center location. These trials lasted 7,000 ms.

PARADIGM 4: ACTIVE PROPRICEPTION WITH VISUAL MEMORY. This task was similar to paradigm 3 except that the handheld peripheral target was flashed again for 100 ms after the hand plate was stopped at an end-stopper, precisely 2,500 ms after the central fixation LED was extinguished and 1,000 ms before the saccade beep instruction (Figs. 2D and 3D). This produced a memory delay of 900 ms between the peripheral visual flash and the saccade, comparable with the memory delay in the visual memory control (paradigm 2).

PARADIGM 5: PASSIVE PROPRICEPTION. This task was similar to paradigm 3 [active proprioception (AP)], but here, the subject's hand was moved passively by the experimenter (Figs. 2C and 3E). The experimenter received a computer-generated voice command through headphones (inaudible to the subject) to move the hand along one groove to the stopper. This movement was accomplished manually using a handle attached to the subject's hand-rest plate.

PARADIGM 6: PASSIVE PROPRICEPTION WITH VISUAL MEMORY. This task was similar to paradigm 4 except that the hand was moved passively as in paradigm 5 (Figs. 2D and 3F).

FIXATION CONTROL. Subjects fixated illuminated LEDs at each of the 16 target locations for 2 s. These fixation controls established the appropriate gaze directions for each target and ensured a standard calibration across the two sessions.

Subjects were provided with a short practice session 1 day before the experiment to familiarize themselves with the tasks and instructions. Data collection was limited by the time allowed to safely wear scleral search coils (~30 min). Each paradigm comprised 80 trials (5 trials \times 16 targets), and a 30-s rest was provided between paradigms to instruct subjects about the next paradigm. The six paradigms were implemented in two sessions: session 1 included the following sequence: AP, AP + visual memory (VM), and a fixation control at the end; session 2 included: passive proprioception (PP), PP + VM, memory saccade (MS), visual saccade (VS), and a fixation control. Paradigms involving visual signals (AP + VM, PP + VM, VS, and MS) were always performed after the proprioceptive-only paradigms to avoid unintentional memorization of the targets, and subjects were provided with no feedback about their performance during the experiment.

The sources of information about target location during these conditions, which include proprioceptive and tactile feedback, limb efference copy signals, and visual signals, are summarized in Table 1. In brief, proprioceptive information was derived from the receptors in the limb muscles, joints, and skin, and visual information was derived from retinal stimulation (from the flashing LEDs). Again, in the proprioceptive tasks (AP and PP), subjects were instructed to wait for an auditory beep and make a saccade to the extinguished LED target,

which was held between the thumb and index finger of the right hand. This LED target also flashed at the final hand position in the combination paradigms (AP + VM and PP + VM).

Calibration and data analysis

The Optotrak system was calibrated according to the manufacturer's instructions. Eye-coil signals were precalibrated using a method that has been described previously (Tweed et al. 1990). This initial calibration was further adjusted by aligning average fixation directions with the actual directions of the 16 target directions (Fig. 2B), calculated from the known locations in space and the measured distance and angles of the subject's eyes from the center of the target display. The search coil provided a 2-D orientation signal relative to the head upright straight-ahead position. To convert these parameters in the standard "oculomotor coordinates," we rotated these signals by the opposite amount of the measured downward orientation of the head (Fig. 2A), which resulted in 2-D gaze vectors defined relative to the frontal plane of the face (Figs. 3 and 4).

To evaluate gaze accuracy with respect to hand position in a common coordinate system, we also transformed the eye orientation signals into "table coordinates." This was done by calculating the intersection point between the line of gaze and the plane of the table top on the level of the LED targets. The result was gaze coded in a Cartesian coordinate system aligned with the forward and lateral axes of the table top. Because our objective was to evaluate the role of arm proprioception in guiding saccades and to compare gaze and hand position, most of our quantitative analysis on saccade accuracy was performed in this coordinate system (Figs. 5–10).

We removed all trials where subjects did not move their eyes or hand, where they did not move their hand in the correct direction, or if the hand did not reach the stopper. For data analysis, saccade onset was defined to be the time at which the velocity of the primary saccade rose above 30°/s, and the final saccade endpoint was defined as the eye position 400 ms after the primary saccade, no matter how many corrective saccades subjects made (typically 0 or 1). Quantitative analysis of saccade accuracy was performed on the final eye position (after corrective saccades) as defined above.

Because we did not provide a constant central fixation after the first 500-ms central fixation stage, eye position often drifted (with small saccades) before the beginning of the main saccade, especially in paradigms when the arm moved (Fig. 3). Because this deviation was caused by a series of small saccades, we called this "microsaccadic drift." To account for this in our analysis, we defined the vector of microsaccadic drift as the difference between the initial position of the eye when the LED was extinguished, and the eye position before the primary saccade. Correlations were calculated using Pearson correlation, and two-tailed pairwise *t*-test with Bonferroni corrections was used (Graphpad Prism Software, San Diego, CA, USA). Factors were analyzed using one-way repeated ANOVAs, followed by a Newman-Keuls post hoc tests.

Optimal inference model

To determine how the brain combines visual and proprioceptive information in our combined proprioception and visual tasks, we built

TABLE 1. Sources of information about target locations

Paradigms	Efference Copy	Visual Signal	Proprioception + Tactile Sensation
Visual saccade	x	✓ (No memory delay)	x
Memory saccade	x	✓ (With memory delay)	x
Active prop.	✓	x	✓
Active prop. + visual mem.	✓	✓	✓
Passive prop.	x	x	✓
Passive prop. + visual mem.	x	✓	✓

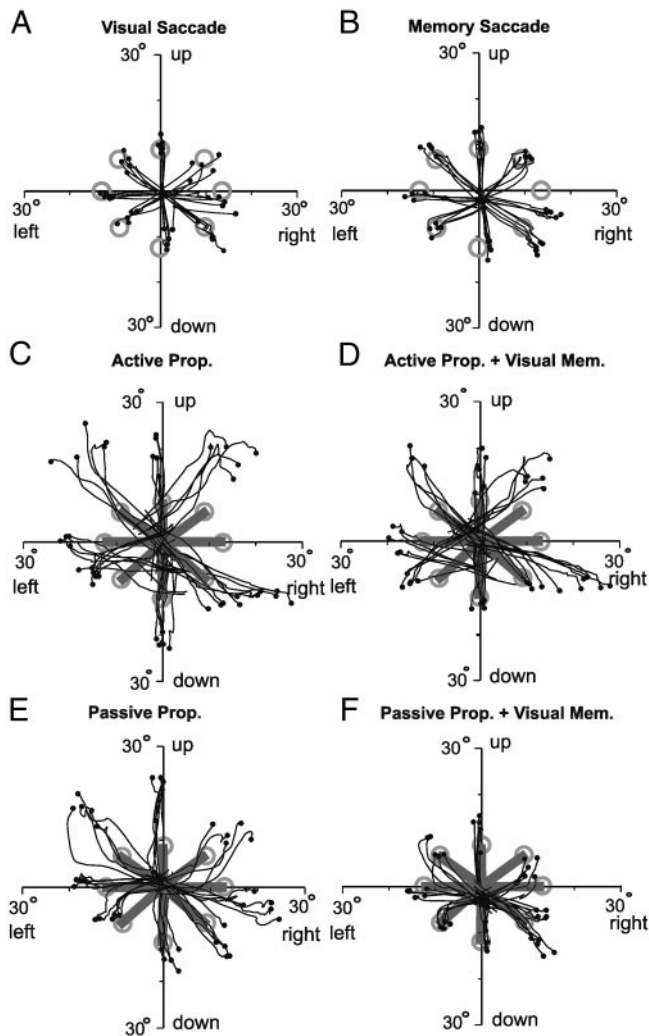


FIG. 4. Sample data from a typical subject: 2-dimensional saccade (black traces) and hand movement (gray traces) trajectories plotted in oculomotor coordinates. For each of the paradigms (A–F), 5 movements are shown to each of the 8 far targets to qualitatively show intraindividual variability and task-dependent saccade accuracy. A: VS task. B: MS task. C: AP task. D: AP + VM task. E: PP task. F: PP + VM task. Empty circles, target locations; black lines, saccade trajectories; filled circles, saccade endpoints; gray lines, trajectory of hand movement. Saccade trajectories did not always begin at center because of microsaccadic drift after extinction of center LED, particularly in hand movement paradigms.

a sensory integration model based on the Bayesian Optimal Inference principle (equivalent to the Maximum Likelihood Estimation or the Minimum Variance Method). This model was used to quantify our behavioral findings by estimating saccade amplitude along the radial direction from the visual (*V*) and (active or passive) proprioceptive (*P*) information available. This was carried out for each condition and each target separately. The equations for this model are provided in the APPENDIX.

RESULTS

Saccade trajectories in oculomotor coordinates

Each of the six subjects successfully performed all six tasks with the proper timing and kinematics, except that they often showed microsaccadic drift during the initial memory interval, especially in the tasks that involved arm movements (Fig. 3).

Figure 4 shows examples of 2-D saccade trajectories toward the eight far targets (○) and a typical pattern of endpoint errors (●) in one subject. Not surprisingly, visually guided saccades (VS) were highly accurate (Fig. 4A). Visual memory–guided saccades (MS) were only slightly more hypermetric and variable (Fig. 4B). Figure 4, C and D, shows saccade trajectories from the active proprioception task without a visual cue (AP) and with visual cue (AP + VM), respectively. In the AP task, saccades were highly hypermetric (Fig. 4C), overshooting the target much more, and with much greater variability than in the MS paradigm. This overshoot was somewhat reduced when an additional visual cue was provided (Fig. 4D), but not to the level of the MS paradigm. Note that in these active proprioception tasks, as well as the passive proprioception tasks shown in the *bottom two panels* of Fig. 4, saccades did not begin perfectly from center because of the microsaccadic drift described above.

Finally, Fig. 4, E and F, shows saccade trajectories during the passive proprioception (PP) and passive proprioception with visual cue (PP + VM) paradigms. These trajectories showed the same trends as observed in the active proprioception tasks. Saccades were more hypermetric in paradigm PP

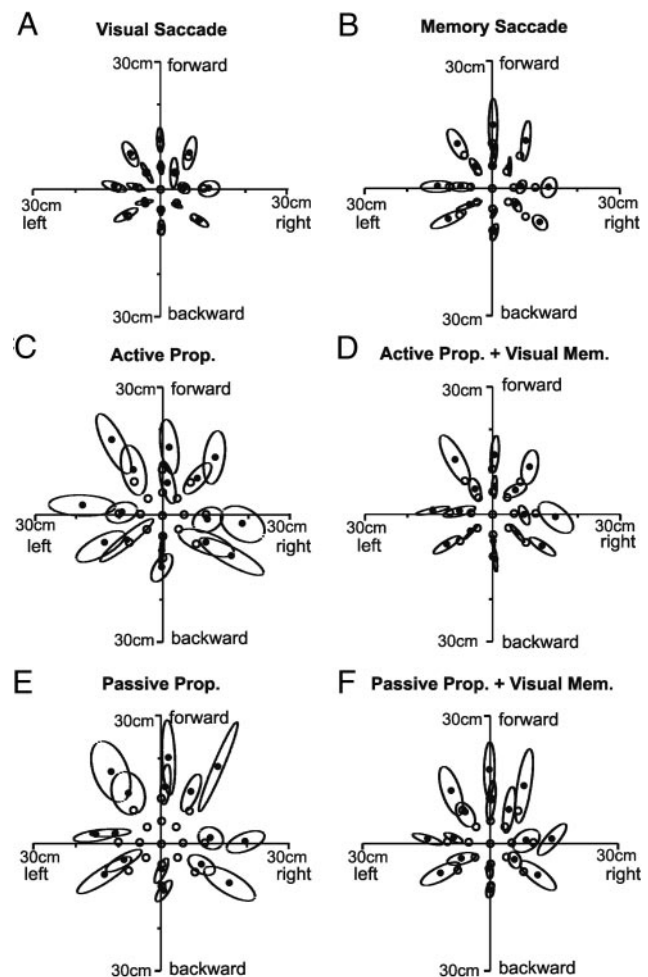


FIG. 5. Error distributions of average saccade endpoints between subjects. Data were represented in 2-dimensional table coordinates and fit with the 68% CI ellipses plotted here. A: VS paradigm. B: MS paradigm. C: AP paradigm. D: AP + VM. E: PP paradigm. F: PP + VM. Empty circles, target locations; filled circles, mean saccade endpoint (across subject means); black unfilled ellipses, error distribution with 68% CI across subjects.

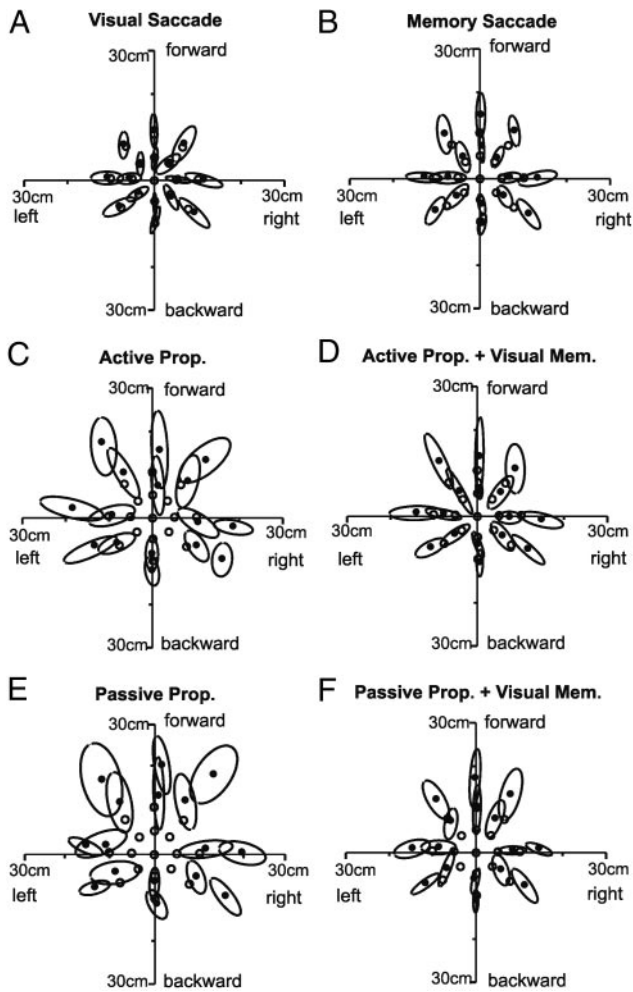


FIG. 6. Error distributions of saccades within subjects. Distribution ellipse was fit to each subject's saccade endpoints in table coordinates, and these ellipse parameters were averaged across the 6 subjects to provide the ellipses plotted here. *A*: VS paradigm. *B*: MS paradigm. *C*: AP paradigm. *D*: AP + VM. *E*: PP paradigm. *F*: PP + VM. Empty circles, target locations; filled circles, mean saccade endpoint; black unfilled ellipses, error distribution with 95% CIs of intrasubject variability, averaged across subjects.

than in paradigm PP + VM, and saccades in both of these paradigms were less accurate and more variable than in the memory saccade paradigm (MS). The following sections quantify these and other observations in much greater detail.

Effect of initial eye position

As noted above, eye position tended to deviate from the center during the initial memory interval, especially in the tasks that involved hand movements. Because this deviation included many small saccades, we called it microsaccadic drift. In theory, the saccade generator should know about these changes in eye position (Becker and Jürgens 1979; Mays and Sparks 1980; Klier and Crawford 1998) and therefore take them into account when calculating the main saccade, but it is still possible that they influenced the pattern of saccade endpoint errors. To test this possibility, we performed multiple linear regression analyses to test the effects of microsaccadic drifts on final saccade errors. As shown in Table 2, we found that, first, the relationship between saccade errors and micro-

saccadic drifts was only significant for the horizontal component of the saccade errors in the AM, AP, PM, and PP paradigms and not for the vertical component or for any component of the VS or MS paradigms. Second, within the horizontal component of these four paradigms, we also found a significant relationship between saccade errors and target locations, and the slope and r^2 values for this relationship were much higher than those seen in the comparison between saccade errors and microsaccadic drifts. Third, the Pearson correlation between microsaccadic drift and target location was also quite high in the preceding four conditions (-0.440 to -0.719). We observed that, in these proprioceptive tasks, these microsaccadic drifts tended to be in the opposite direction as the hand movement that was directed to a target position. Therefore target position and microsaccadic drift are both related to the hand movement direction.

We therefore used multiple linear regression to disentangle the relative contributions of target location and microsaccadic drift on saccade error. We found that, although there were significant r^2 changes when adding the microsaccadic drift as an independent variable into the equation already containing target position ($P < 0.05$, $n \approx 480$; see Table 2), the actual contribution of microsaccadic drift to saccade error was quite

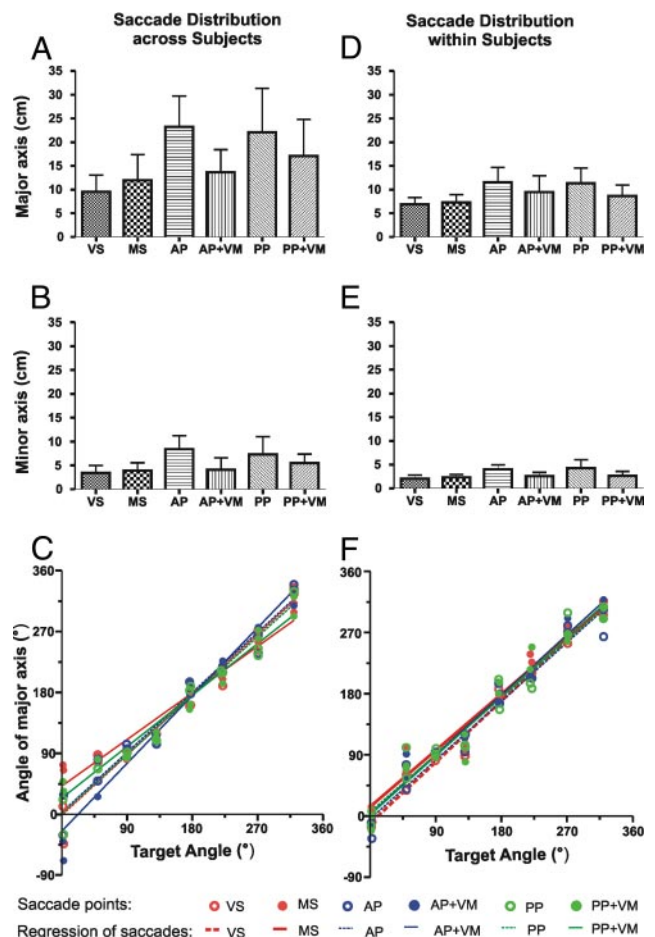


FIG. 7. Saccade error distribution: parameters from 95% CI ellipses. Bars show parameters averaged across targets and across subjects (\pm SD) for both intersubject variability (left column) and intrasubject variability (right column). Top row: lengths of major ellipse axes. Middle row: lengths of minor axes. Bottom row: scatter plots (\circ) and linear regressions of the major-axis angles as a function of the target location angles.

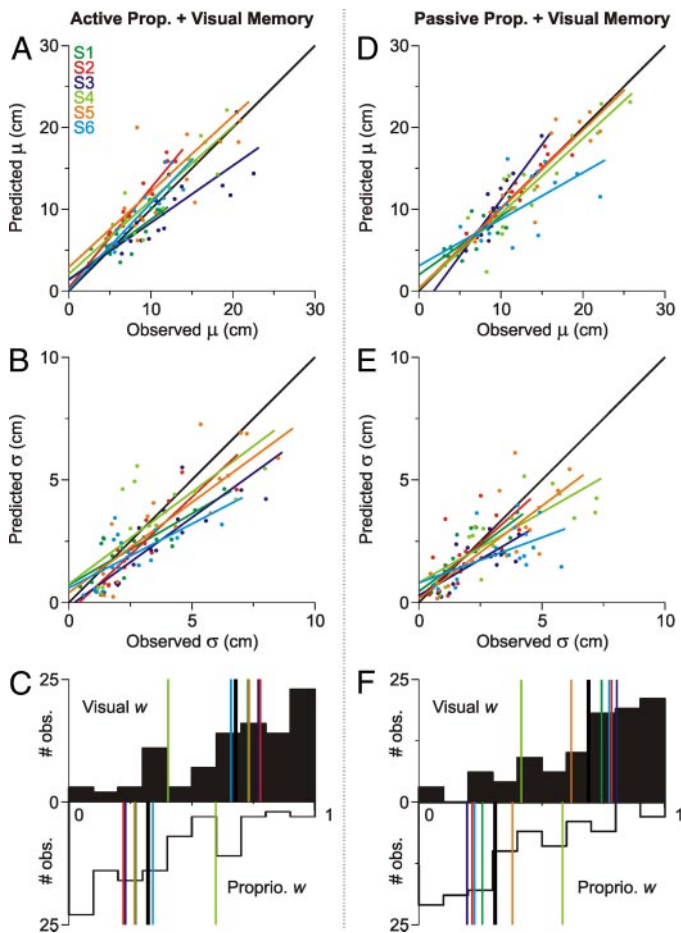


FIG. 8. Comparison between optimal inference model predictions and data. Each data point corresponds to one target. Data and regression lines for all 6 subjects are shown. A perfect prediction of the data by the model would yield a slope = 1 (black lines). *A* and *B*: predicted location (mean, μ , *A*) and variability (SD, σ , *B*) of target location for combined active proprioception and visual memory task (AM). *C*: relative weights of visual (black) and proprioceptive (white) information for AM. Histograms show number of weights within each bin (width = 0.1) for each target position across all subjects. On the x-axis, weight = 0 means that this variable is not used at all; weight = 1 means that the optimal estimate only relies on this variable. Solid black lines are population means (visual = 0.68, proprioception = 0.32); other colored lines are means for individual subjects (visual = 0.40...0.78, proprioception = 0.22...0.60). *D* and *E*: location (mean, μ , *D*) and variability (SD, σ , *E*) of the predicted target location for passive proprioception and visual memory (PM) task. *F*: relative weights for PM. Population means (visual = 0.69, proprioception = 0.31) and means for individual subjects (visual = 0.42...0.80, proprioception = 0.20...0.58).

small, only accounting for 0.1–3% (r^2 changes when adding microsaccadic drift to the equation) of the variability in saccade error (r^2 changes were significant basically because of the large number of trials: $n \approx 480$). Thus we conclude that microsaccadic drift does not account for the final saccade error patterns seen in our tasks. These results suggest that deviations in initial eye position provided only a very minor contribution to the amplitude and direction of the saccade errors, especially compared with the highly task-dependent factors described below.

Gaze accuracy in table coordinates

To quantify the pattern of saccade errors, we plotted the data from each of the six paradigms in table coordinates: a Cartesian

coordinate system aligned with the forward–backward and transverse axes of the target board (Figs. 5 and 6). Our quantification confirmed the qualitative observations noted above. Absolute errors of saccades were significantly different among the paradigms ($F_{(5,75)} = 6.55$, $P < 0.0001$). Specifically, saccades made immediately toward a visual target (VS) were significantly more accurate than saccades made after a short memory delay (MS; $P < 0.01$). Saccades in MS were significantly more accurate than the saccades made in the paradigms of proprioception only tasks (AP and PP) and passive proprioception with visual information (PP + VM; all $P < 0.01$). In contrast, although there was a trend for MS saccades to be more accurate than saccades made to handheld targets that were briefly seen after the hand was actively moved (AP + VM), this trend was not significant ($P = 0.254$). Furthermore, saccadic movements during AP + VM were significantly more accurate than those during AP ($P < 0.001$), and saccades made during PP + VM were significantly more

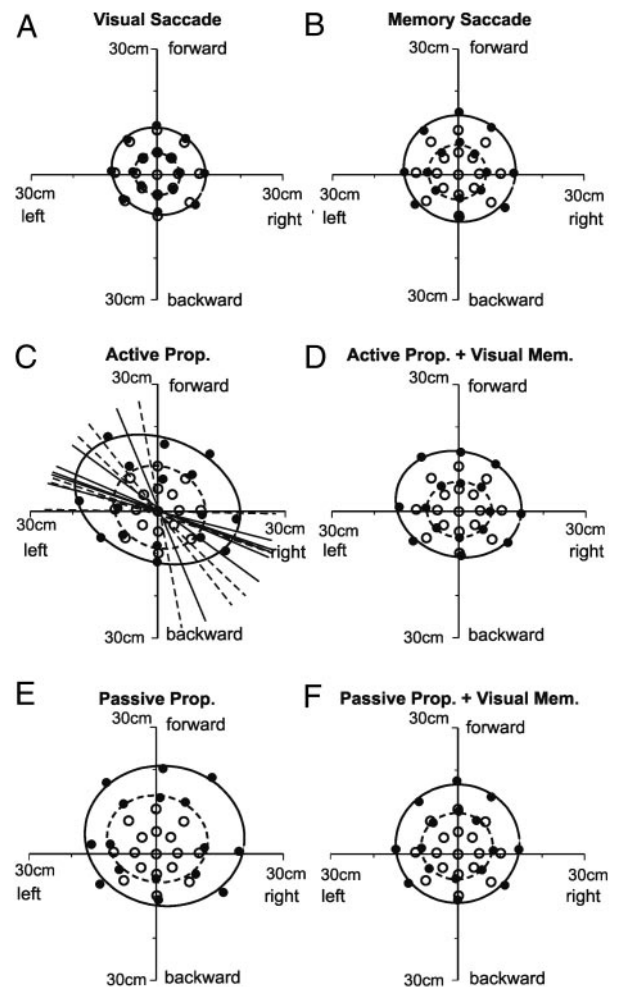


FIG. 9. Shape of overall saccade error patterns. Ellipses were fit to the overall saccade endpoints (across all subjects) for the near target locations and for the far target locations, respectively, in table coordinates. *A*: VS task. *B*: MS task. *C*: AP task. This panel also shows directions of major ellipse axes for each individual. *D*: AP + VM task. *E*: PP task. *F*: PP + VM task. Empty circles, target locations; filled circles, overall mean saccade endpoints; dashed-line ellipses, fit to saccades for near targets; solid-line ellipses, fit to saccades for far targets; dashed lines in *C*, directions of major axis of far-target ellipses for each subject; solid lines in *C*, direction of major axis of near-target ellipses for each subject.

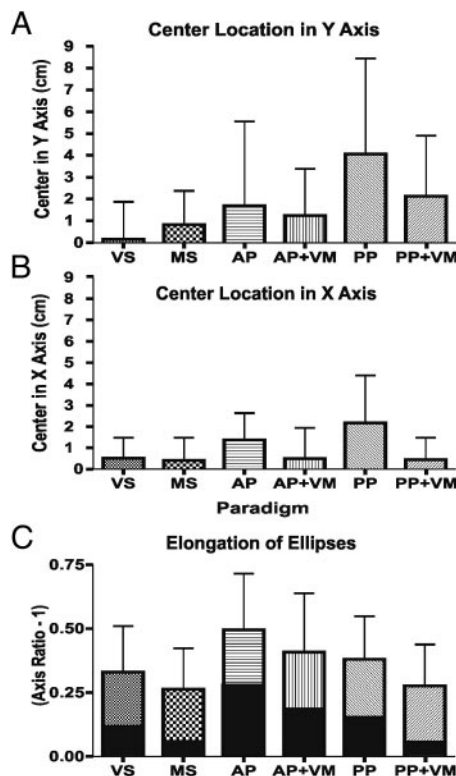


FIG. 10. Shift and elongation parameters of the error pattern ellipses (like those in Fig. 9) fit to individual subjects. Bars show averages between fits to near and far targets, averaged (\pm SD) across subjects ($n = 12$). *A*: shifts of ellipse centers along the y -axis (forward–backward) of table coordinates. *B*: shifts of ellipse centers along the x -axis (leftward–rightward) of table coordinates. *C*: elongation scores of ellipses. These scores were calculated and plotted for each paradigm. Pattern-filled bars, average (\pm SD) values of the elongation scores from each individual subject; superimposed black bars, elongation scores of the overall average near-target and far-target ellipses shown in Fig. 9.

accurate than those during PP alone ($P < 0.01$). Thus saccade accuracy was significantly increased with visual information, and saccades made toward a nonvisual target moved by the hand (AP and PP) were least accurate, as shown qualitatively in Figs. 5 and 6.

TABLE 2. Multiple linear regression

Condition	Direction	Model 1 Slope (r^2 , P)	Model 2 Slope (r^2 , P)	Pearson Correlation (Between IVs)	Model 3			change P
					r^2	Slope 1	Slope 2	
VS	H	0.299 (0.089*)	0.258 (0.047)	0.006	0.155	0.297	0.256	0.066*
	V	0.106 (0.011)	0.199 (0.040)	-0.051	0.053	0.116	0.213	0.042*
MS	H	0.685 (0.469*)	0.126 (0.016)	-0.036	0.492	0.690	0.150	0.023*
	V	0.477 (0.228*)	0.268 (0.042)	0.027	0.303	0.470	0.274	0.075*
AP	H	0.623 (0.389*)	-0.438 (0.192*)	-0.440	0.422	0.534	-0.203	0.033*
	V	0.466 (0.217*)	0.006 (0.000)	-0.284	0.238	0.509	-0.151	0.021*
AP + VM	H	0.667 (0.446*)	-0.568 (0.322*)	-0.719	0.461	0.537	-0.182	0.015*
	V	0.374 (0.140*)	-0.072 (0.005)	-0.393	0.146	0.408	-0.088	0.006*
PP	H	0.759 (0.576*)	-0.438 (0.192*)	-0.534	0.577	0.734	-0.046	0.001†
	V	0.597 (0.357*)	-0.037 (0.001)	-0.229	0.367	0.621	0.105	0.010*
PP + VM	H	0.666 (0.443*)	-0.393 (0.154*)	-0.539	0.445	0.640	-0.048	0.002†
	V	0.472 (0.223*)	0.032 (0.001)	-0.357	0.269	0.554	0.229	0.046*

Model 1: the DV is saccade error, the IV is target location. Model 2: the DV is saccade error, the IV is microsaccadic drift. Model 3: the DV is saccade error, the IVs are target location and microsaccadic drift. H: Horizontal component; V: Vertical component. * $P < 0.05$; † $P \geq 0.05$. DV, dependent variable; IV, independent variable; VS, visual saccade; MS, memory saccade; AP, Active proprioception; VM, visual memory; PP, passive proprioception; H, horizontal component; V, vertical component.

To characterize the systematic accuracy of saccades and its variability between subjects in table coordinates, we fitted 68% CI ellipses to the distribution of the average saccadic responses of each subject (Fig. 5). In terms of accuracy, subjects performed most consistently in the vision-only tasks, i.e., with the smallest intersubject variation (Fig. 5, *A* and *B*). In contrast, the distribution of saccade endpoints was largest in the nonvisualized proprioceptive updating tasks (Fig. 5, *C* and *E*), with intermediate levels of variation in the tasks combining visual memory and proprioception (Fig. 5, *D* and *F*). Moreover, intersubject variability was greatest in the radial direction of eye and arm movement (the long axis of an ellipse).

To show the intraindividual variability (precision) of the saccades, we fitted 95% CI ellipses to the saccade endpoints of each subject and averaged the parameters of these ellipses across subjects, including the length of the major and minor axes and the direction of the major axis (Fig. 6). This showed that intrasubject variability was largest in the nonvisual paradigms (Fig. 6, *C* and *E*), intermediate in the combined sensory paradigms (Fig. 6, *D* and *F*), and lowest in the vision paradigms (Fig. 6, *A* and *B*). Again, the main source of variability within subjects (the long axes of the ellipses) was along the radial direction in all paradigms.

To quantify the error distribution across subjects and within subjects, we calculated the lengths of the major and minor axes of the saccade endpoint ellipses (now calculated from 95% CIs for both inter- and intrasubject variability). Overall, the saccade distributions were broader across the subjects (Fig. 7, *A* and *B*) compared with those within the subjects (Fig. 7, *D* and *E*). In all cases, the length of the long axis was significantly different from the length of the short axis ($P < 0.01$), and on average was 1.36 times greater. However, there was no significant difference among the paradigms in the ratio between the long and the short axes of the ellipses for 16 targets in the across-subject analysis ($F_{(5,75)} = 1.28$, $P = 0.28$). There was only a significant difference in this ratio for the AP and AP + VM paradigms ($P < 0.05$) in the within-subjects analysis ($F_{(5,75)} = 3.00$, $P < 0.0001$). Thus, with this one exception, the tasks did not affect the shape of the error distribution, only the size of the error distribution.

What was the orientation of these ellipses? To quantitatively confirm our observation that the long axes of the error ellipses were aligned with target directions (i.e., the direction of saccades and hand movements), we defined the rightward direction of the horizontal axis in the table coordinates (Figs. 5 and 6) as 0° (in a radial coordinate system). The coordinate system was based on a counterclockwise rotation from 0 to 360° . In this way, we defined the right, up-right, up, up-left, left, down-left, down, and down-right target locations as $0, 45, 90, 135, 180, 225, 270,$ and 315° , respectively. The basic ellipse fitting algorithm provided the orientations of the major axes of ellipses between 0 and 180° (because one cannot distinguish between an ellipse orientation of 0 and 180°). To correct for target locations $>180^\circ$, we added 180° to the final orientations of the corresponding ellipses. The *bottom row* of Fig. 7 shows these angles for the major axes of saccade error distributions as a function of the angles of target locations, both across subjects and within subjects. The orientation of the long axes of the error ellipses increased linearly as a function of target direction in both the across-subject (Fig. 7C) and within-subject distributions (Fig. 7F). The average slope for across-subject distributions was 0.94 ± 0.12 (SD) (Fig. 7C), and the average slope for within-subject distributions was 0.95 ± 0.03 (Fig. 7F). The angle of the major axis of ellipsis was highly correlated with target angle in both the across-subject data ($r = 0.96 \pm 0.01$) and in the within-subject data ($r = 0.967 \pm 0.01$) paradigms.

Thus in all tasks, saccades were more accurate and precise in their direction than in their amplitude. This pattern suggests a dissociation between the control of the direction and amplitude of saccades, as shown previously in reaching movements by Messier and Kalaska (1997), and in visually guided saccades (Niemeier et al. 2003).

Weighting of visual and proprioceptive inputs in the combination tasks

In the AP + VM and PP + VM paradigms, subjects used both visual and proprioceptive inputs to update target representations for saccades. To study how these different inputs were weighted, we built an optimal inference model (see METHODS and APPENDIX; Fig. 8). We tested this model and showed that it predicted the data well both for the constant (Fig. 8, A and D) and variable errors (Fig. 8, B and E). The close match between this simple optimal signal combination model and the observed data occurred despite the few number of trials for each target ($n = 5$).

We analyzed the different weights of visual and proprioceptive signals in Fig. 8, C and F. Weight = 0 means that the variable was not used in the estimate at all, and weight = 1 means that the estimate relied completely on this one variable. In the AP + VM paradigm, the average weight of visual signal was 0.68 (range for individual subjects: 0.40–0.78), and the average weight of proprioceptive feedback was 0.32 (range for individual subjects: 0.22–0.60). In the PP + VM paradigm, the average weight of visual signal was 0.69 (range: 0.42–0.80), whereas the average weight of proprioceptive feedback was 0.31 (range: 0.20–0.58). There was no significant difference in the multisensory weighting between the active and passive hand movement paradigms. Thus, in these proprioceptive + visual tasks, it seems that, although visual information plays a greater role in determining the location of the saccade goal

compared with proprioceptive information, proprioceptive information is not completely overwritten by the visual information.

Coordinate systems and sources of error

To test the coordinate system(s) in which the error patterns arose, we studied the effect of target direction on amplitude errors for each paradigm. To do this, we fitted ellipses to the averaged across-subject saccade endpoints separately for the eight near targets and eight far targets for each task (Fig. 9). Despite the symmetrical circular distribution of the targets, the distribution of average saccade endpoints showed distinctive patterns in the different paradigms. The ellipses for the visual paradigms (VS and MS) appeared to align symmetrically around the central point (Fig. 9, A and B), whereas in all of the proprioception and proprioception plus vision paradigms, there was a shift of saccade endpoints away from the subjects' bodies (Fig. 9, C–F), especially in the passive proprioception paradigm (PP; Fig. 9E).

In the vision-only tasks (Fig. 9, A and B) and in the PP + VM tasks (Fig. 9F), the elliptical fits appeared to be nearly circular, but in the other tasks (Fig. 9, C–E), the elliptical fits were somewhat elongated. In the AP + VM and PP tasks (Fig. 9, D and E), the ellipses were only slightly elongated with a slight tilt. However, the active proprioception ellipses (Fig. 9C) showed both a greater elongation and a greater tilt in the direction predicted by errors in a proprioceptive coordinate system, with larger errors in the flexion–extension axis (Fig. 1A). These tilts were also observed in individual subjects, as shown by the plots of the long axes of ellipses fit to individual data, superimposed in Fig. 9C. These patterns of shifting and tilting are consistent with the idea of an anisotropy in hand inertia (Gordon et al. 1994; Hogan 1985).

To quantify the displacement of the centers of overall saccadic ellipses (Fig. 9) from the center of the table coordinates, we analyzed the distributions (mean \pm SD) of the averaged position of the centers of the two ellipses from each individual (Fig. 10). Only the centers of the PP and PP + VM ellipses were shifted significantly from the target center ($P < 0.05$) along the y (forward) axis. Only the center of the average PP ellipse was significantly displaced from zero ($P < 0.01$) along the x (transverse) axis. Therefore the passive proprioception tasks (PP) showed the largest shift, where the center of ellipses of errors shifted significantly forward and rightward compared with visually controlled tasks (VS and MS). In addition, there was a significant difference ($P < 0.05$) in the center location on the y -axis between AP (1.69 ± 3.87 cm) and PP (4.06 ± 4.39 cm). There was no significant difference ($P = 0.144$) in the center location on the x -axis between AP (1.37 ± 1.26 cm) and PP (2.17 ± 2.24 cm). There was no significant difference ($P = 0.070$) in the elongation of ellipses between AP (0.50 ± 0.22) and PP (0.38 ± 0.17).

To quantify the task-specific alteration of the coordinate frames for saccade errors (Fig. 1), we first characterized the elongation of the ellipses. There is an inherent computational problem with determining the tilt: the closer the ellipse is to being circular, the less certain the measure of tilt is and the more the data are subject to noise. To determine if a given ellipse was sufficiently elongated, we applied the following formula

$$\text{Elongation} = (\text{long axis}/\text{short axis}) - 1$$

This provides both a measure of elongation and also a certainty score for measuring ellipses ranging from zero (circular ellipse) to infinite certainty (a line). We judged that ellipses that were significantly elongated relative to the visual paradigms (VS and MS) could be reliably used to judge the tilt of the overall error distribution in the proprioceptive updating tasks.

Elongation scores for all subjects (mean \pm SD) and two fitted ellipses (near and far targets) were calculated ($F_{(5,55)} = 3.95$, $P < 0.05$) and plotted in Fig. 10C. Note that this score does not average linearly to equal the score for the overall average data (superimposed black bars) derived from the plots in Fig. 9. The overall score is lower because individual subjects show elongations in different directions that tend to cancel out in averaging. However, both measures show the same pattern, i.e., that the AP paradigm produced the greatest elongation. The PP task showed an intermediate elongation, whereas the addition of a visual cue in the AP + VM and PP + VM paradigms reduced elongation in both tasks. Importantly, the elongation score for the AP task was the only score that was significantly different from both the nonproprioceptive VS ($P < 0.05$) and MS ($P < 0.01$) paradigms. For this reason, we concluded that the AP ellipses provided the only reliable measure of ellipse rotation in the proprioceptive tasks.

We next examined the tilt of the AP ellipses to determine if they were significantly rotated toward a limb/joint coordinate system. For reference, the average (across subjects) angle between the line of the forearm (at the center resting position) and the leftward direction of the horizontal axis in table coordinates was 42.05° . The average rotations of the major axes of the ellipses fit to the saccade endpoints in AP condition for individual subjects were $30.05 \pm 19.73^\circ$ for the outer ellipse (plotted as lines in Fig. 9C) and $35.18 \pm 28.47^\circ$ for the inner ellipse (compared with 24.68 and 21.29° , respectively, for the ellipse fits to overall average data that are shown in Fig. 9). These rotations (for individual subjects) were significantly greater than zero ($P = 0.003$), but were not significantly different from the angle of forearm ($P = 0.287$). For comparison, the mean overall rotations of the AP + VM, PP, and PP + VM tasks (which did not meet our tests for reliability) were 7.99 , 9.35 , and -3.88° , respectively. We found no significant correlations between the tilt of these ellipses and the direction of the shifts shown in Fig. 10, A and B. In summary, the AP paradigm was the only condition that produced significant elongation of the overall error pattern relative to the visual only paradigms, and these ellipses were rotated by approximately two thirds the angle of the forearm at its resting position.

DISCUSSION

Our results show several new findings: First, somatosensory information can be used to update the internal representation of handheld target locations for saccades. However, these somatosensory-based saccades are much less accurate and less precise than visually guided or visual memory saccades. Additional visual cues improved performance, but the reverse was not true, i.e., additional somatosensory inputs not only failed to improve on the vision-only tasks; they even degraded the performance. These sources of somatosensory error equally increased the variability of saccade amplitude and direction,

with amplitude always greater than direction. Reliance on somatosensory input also produced systematic (average) errors: saccades were hypermetric in all directions, but especially so in the forward (away from the body) and rightward directions. Furthermore, saccade hypermetria was most pronounced along an axis rotated toward the arm flexion–extension direction in the active proprioception task.

Spatial updating

We found that the saccade generator can use proprioceptive feedback from the limb to update handheld target locations. Such an updating facility would be useful, for example, for keeping track of the location of a handheld tool while one redirects gaze toward other potential objects of interest. This shows that there is an interplay between the eye and hand systems not only in the usual visuomotor eye-to-hand sense, but also in the reverse hand-to-eye sense (Nanayakkara and Shadmehr 2003; Scheidt et al. 2005). Such two-way communication between the limb system and oculomotor–visual system is probably important when subjects are engaged in complex, natural eye–hand coordination tasks (Johansson et al. 2001).

Updating across gaze movements of the eyes, head, and body has been observed in many visual memory tasks (Bloomberg et al. 1988; Hallett and Lightstone 1976; Israel and Berthoz 1989; Maurer et al. 1997; Mays and Sparks 1980; Medendorp et al. 2003; Mergner et al. 1992, 1998; Pelisson et al. 1989). In these experiments, the updating problem arose because self-generated eye motion changed the location of the sensor (the retina) relative to a space-fixed target, whereas in the current experiment, the updating problem arose because self-generated motion of the arm changed the location of the target relative to a space-fixed retina. In either case, the fundamental updating problem occurs because some type of self-motion changes the spatial relationship between the remembered target and the sensor, and both of these problems could occur simultaneously in natural eye–hand coordination tasks.

Error patterns in proprioceptive updating

Four paradigms (AP, AP + VM, PP, and PP + VM) in our experiment involved composite actions of both the eye and the hand. Therefore the sources of errors in these paradigms may have derived from the eyes, the hand, or both. In our visual tasks, not surprisingly, the pattern of errors can be explained simply within an eye- or head-centered coordinate system. However, in nonvisual tasks (PP and especially AP), the errors of saccades showed a pattern that was suggestive of a body, limb, or joint coordinate system (Nanayakkara and Shadmehr 2003). First, saccades were more hypermetric toward far targets than toward near targets, especially in the passive proprioception task, producing an overall shift in the saccade error pattern away from the body (i.e., the forward and rightward shift of the ellipses in Fig. 9). Second, in the active proprioception task, the overall pattern of errors was elongated along an axis that was tilted toward the flexion–extension axis of arm movement.

It is possible that some of the errors observed in the proprioceptive tasks derive directly from errors specific to the

proprioceptive system (Van Beers et al. 1998, 2002b). However, this does not explain why the errors in the saccade task are so much larger than errors observed in other tasks requiring accurate limb proprioception (Henriques and Soechting 2003; Van Beers et al. 1998, 2002a). These seem to be specific to proprioceptively guided saccades. Therefore the observed hypermetria of the saccades might be caused by an imperfect calibration of proprioceptive signals used to remap the target. This seems to be a reasonable assumption given that, in everyday life, proprioceptive signals are normally overwritten by visual information (spatially more accurate). Moreover, the errors specific to the proprioceptive system do not account for the differences observed between the active and passive proprioceptive tasks.

Therefore, although we did not measure the axes of limb inertia in the experiment, the saccade error patterns that we observed seem to be consistent with previous reports of directional anisotropy in limb inertia (Gordon et al. 1994; Hogan 1985). This suggests that in the proprioception tasks, especially the active proprioception task, a predominant source of saccade error originated from joint or limb-centered coordinates. The specific reasons for these errors will be discussed when we consider the neurophysiology of these eye–hand systems.

Sensory integration and target representation

Recent studies have suggested that the senses usually provide redundant information, and when integrating redundant signals, the brain forms a statistically optimal (i.e., minimum variance) estimate by weighting each modality according to its relative precision. Minimum variance models have been shown to account for human performance when subjects integrate vision and touch (Ernst and Banks 2002), vision and audition (Battaglia et al. 2003), and other combinations of sensory input (Jacobs 1999; Van Beers et al. 1999; Welch et al. 1979). Similarly, in our AP + VM and PP + VM tasks, subjects received both visual and proprioception (afferent and/or efferent proprioceptive signals) estimates of the target location. The integration of visual and proprioceptive information has been studied extensively (Haggard et al. 2000; Plooy et al. 1998; Welch 1978; Welch and Warren 1986). In our experiment, most of the errors associated with proprioception were significantly reduced when an additional visual cue was provided, even after a memory interval. This seems to be an example of the brain weighting different inputs according to their reliability (Sober and Sabes 2003; Van Beers et al. 1996).

According to the optimal inference model, the weight of the visual signal was 0.68 in the AP paradigm and 0.69 in the PP

paradigm (thus the complimentary weight of the proprioceptive signal was only 0.32 for AP and 0.31 for PP). This supports the idea that the brain performs an optimal combination of all available sensory information, with visual memory being the more reliable of the two sources. The relative weights were very similar for AP and PP conditions, even on a subject-by-subject basis, presumably because the ratio of reliability between proprioceptive and visual inputs is normally constant in everyday active behavior. In other words, the oculomotor system seems to rely on an internal model of hand position that is derived from both afferent and efferent proprioceptive signals, and being upstream from this model, it is not able to disentangle the earlier inputs. Thus the weighting of visual and somatosensory inputs (Fig. 11, asterisk points at which these inputs are weighted in the optimal inference model) probably occurs at a late stage.

Interestingly, proprioception did not improve on vision alone. Indeed, the Bayesian model says it should not because proprioception was less accurate than vision. Why then weight in proprioception at all? This is likely a product of the memory interval, where visual reliability fades compared with the reliability of sustained proprioceptive inputs; eventually proprioception is better, as in the case where there is no vision at all. The relatively poor performance of the proprioceptive system in guiding eye movements is not entirely surprising, because the primary task of the eye–hand coordination system is to guide hand movements using visual gaze (Abrams et al. 1990; Scheidt et al. 2005), not the other way around. Nevertheless, it is possible that this sense is better calibrated in individuals who work with their hands professionally.

Neurophysiological models for proprioceptive updating of saccades

The eye and hand seem to be controlled by parallel but interacting mechanisms (Snyder et al. 2002). Lazzari et al. (1997) proposed a model in which both motor systems are completely independent but exchange information, mediated by sensory signals (e.g., visual from the eye, proprioceptive from the arm) and efference copies of motor commands. Our experiment identified a new kind of interaction—the spatial updating of handheld target representations in the saccade generator based on proprioceptive feedback from the limb.

Such signals could enter the saccade generator at a number of points, such as the cerebellum, which possesses both oculomotor and limb proprioception signals (Lynch and Tian 2005; Shadmehr 2004). However, our hypothesis is that proprioceptive updating acts at the same early level as the previ-

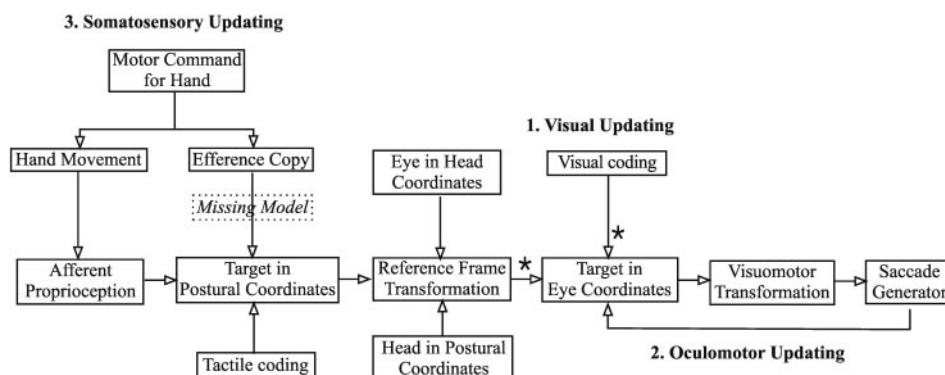


FIG. 11. Proposed model for the spatial updating of handheld targets. Target in eye coordinates representation can be updated based on 1) visual information, 2) movements of the eyes themselves, and 3) somatosensory inputs (including proprioception, tactile sensation, and efference copy of the command of arm movement). Arrows, direction of signal transduction; labeled boxes, key steps in updating process and required transformations; dashed box, missing internal model that we propose explains elongation and tilt of error patterns in AP paradigm; *, points where inputs are weighted in the optimal inference model.

ously observed signals associated with gaze-centered updating across saccades. In other words, we propose that the common buffer for target storage and updating is an eye-centered coordinate system (Anderson and Buneo 2002; Batista et al. 1999; Colby and Goldberg 1999; Duhamel et al. 1992; Henriques et al. 1998; Medendorp et al. 2003). The scheme in Fig. 11 shows how this might occur. The schematic depicts a simple visuomotor transformation for saccades (Crawford and Guitton 1997) and other several means of updating the target location. In brief, the gaze-centered visuospatial memory buffer can receive and synthesize information from 1) the visual system itself; 2) the oculomotor system to update targets in eye-centered coordinates; and 3) the somatosensory updating system. Clearly the latter would require several reference frame transformations to correctly transform proprioceptive signals from limb-based coordinates into gaze-centered coordinates (Buneo et al. 2002).

The latter supposition would implicate a number of cortical and subcortical saccade areas as the targets for proprioceptive updating, including the lateral intraparietal area (LIP) (Duhamel et al. 1992; Medendorp et al. 2003; Nakamura and Colby 2002), the superior colliculus (Nakamura and Colby 2002; Walker et al. 1995), and the frontal eye fields (Heide et al. 2001; Nakamura and Colby 2002; Umeno and Goldberg 1997). Buneo et al. (2002) have recently found evidence that hand position may be represented in gaze-centered coordinates in posterior parietal cortex. Similarly, hand position signals could be used for the calculations required in our tasks. Oculomotor and limb signals are closely associated in parietal cortex (Baker et al. 1999; Batista et al. 1999; DeSouza et al. 2000). Conversely, LIP preferentially encodes targets for upcoming eye movements but also possesses responses related to limb movements (Dickinson et al. 2003; Snyder et al. 1997). Therefore we suggest that the transformations, required for proprioceptive-oculomotor updating, occur through a mechanism similar to that proposed by Buneo et al. (2002) for arm movements, but targeting specifically the saccade-related network in areas like LIP.

Our results from the active proprioceptive tasks suggest that the saccade generator may receive an efference copy that originates from a level at or downstream from primary motor cortex. Recent unit recording experiments suggest that the output of M1 (but not parietal cortex) may compensate for the anisotropy observed in limb inertia (Scott et al. 1997), producing greater discharge for extension-flexion than adduction-abduction (Sergio et al. 2005). If the saccade generator received this command as an efference copy of the limb movement, it would have to transform these anisotropic signals through a "forward model" of limb inertia to correctly calculate the limb kinematics. The error pattern that we observed in the active proprioceptive tasks suggests that the saccade generator does receive such a signal, but fails to completely account for its anisotropy. Consistent with this, this particular pattern of error disappeared in the passive proprioception tasks (i.e., because here there is neither a motor command nor an efference copy of the motor command). The precise directions of the anisotropy in our data do not perfectly match the anisotropies observed in the primate neurophysiological data (Sergio et al. 2005), but this could simply represent a species or task difference. Furthermore, any difference in the saccade anisotropy

and the actual mechanical anisotropy in the human limb could result from a partially, but not properly, calibrated forward model.

Finally, one can see that the variability of saccade endpoints in our experiment is inherent in all saccades, especially in the amplitude. The changes in variability could be caused by noise in the internal estimate of the hand movement vector or in the estimate of the difference between the initial eye position and the target. These two possibilities cannot be disentangled in this study because they were always correlated (i.e., initial eye and hand position were always at center). To distinguish between these possibilities will require further experiments in the future.

To conclude, the saccade generator can update handheld target locations for saccades by using proprioceptive information from the limb. However, proprioceptive input is not as accurate as visual input in guiding saccades. In addition, our results indicate that the saccade generator cannot fully compensate for the anisotropy of limb inertia. During the process of active proprioceptive updating, saccade errors are likely to originate from limb-centered coordinates, a hypothesis that could be confirmed by systematically dissociating these coordinates from other gaze-related coordinate systems. Finally, our proposed model offers potential pathways of the spatial updating of handheld target locations for saccades that may be tested physiologically in the future.

APPENDIX

Optimal inference model

To compute \hat{x} (estimated saccade amplitude) from the available visual (V) and (active or passive) proprioceptive (P) information, we used an optimal inference model (Duda et al. 2001)

$$\hat{x} = \frac{\int dx \times x \times p(x|VP)}{\int dx \times p(x|VP)}$$

$p(x|VP)$ is the probability of the target being at location x , given the visual (V) and proprioceptive (P) inputs. We used standard statistical rules (Duda et al. 2001) to compute $p(x|VP)$ as $p(x|VP) = p(V|x) \times p(P|x) \times p(x)$.

In our case, the prior $p(x)$ was simply a uniform distribution. The conditional probabilities $p(V|x)$ and $p(P|x)$ were Gaussians with independent means (μ_v , μ_p) and noise (σ_v , σ_p). We estimated the parameters of these Gaussians from our data, i.e., from the visual memory (VM) and active or passive proprioception only (AP or PP) conditions. We computed the posterior probability density function $p(x|VP)$ to make predictions for the combined vision and (active or passive) proprioception tasks. Because $p(x|VP) \propto p(V|x) \times p(P|x)$, we calculated the predicted means ($\hat{\mu}$) and SD ($\hat{\sigma}$) for the combined proprioception and visual memory task from the multiplication of the two Gaussians as follows

$$\hat{\sigma}^2 = \frac{\sigma_v^2 \times \sigma_p^2}{\sigma_v^2 + \sigma_p^2} \leq \min(\sigma_v^2, \sigma_p^2)$$

$$\hat{\mu} = \hat{\sigma}^2 \left(\frac{\mu_v}{\sigma_v^2} + \frac{\mu_p}{\sigma_p^2} \right) \in [\mu_v, \mu_p]$$

We also computed the relative weights of the visual and proprioceptive information, i.e., what was the proportion of visual and proprioceptive information used to compute the optimal estimate. These are given by the following expression

$$w_{v|p} = \frac{1/\sigma_v^2}{1/\sigma_v^2 + 1/\sigma_p^2}$$

ACKNOWLEDGMENTS

We thank S. Sun and H. Wang for technical support.

GRANTS

This work was supported by the Canadian Institutes of Health Research (CIHR). L. Ren was supported by the Ontario Graduate Scholarship, A. Z. Khan was supported by an NSERC Postgraduate Award, G. Blohm was supported by a Marie Curie International fellowship within the 6th European Community Framework Program and CIHR (Canada), and J. D. Crawford holds a Canada Research Chair.

REFERENCES

- Abrams RA, Meyer DE, and Kornblum S.** Eye-hand coordination: oculomotor control in rapid aimed limb movements. *J Exp Psychol Hum Percept Perform* 16: 248–267, 1990.
- Andersen RA and Buneo CA.** Intentional maps in posterior parietal cortex. *Annu Rev Neurosci* 25: 189–220, 2002.
- Ariff G, Donchin O, Nanayakkara T, and Shadmehr R.** A real-time state predictor in motor control: study of saccadic eye movements during unseen reaching movements. *J Neurosci* 22: 7721–7729, 2002.
- Baker JT, Donoghue JP, and Sanes JN.** Gaze direction modulates finger movement activation patterns in human cerebral cortex. *J Neurosci* 19: 10044–10052, 1999.
- Batista AP, Buneo CA, Snyder LH, and Andersen RA.** Reach plans in eye-centered coordinates. *Science* 285: 257–260, 1999.
- Battaglia PW, Jacobs RA, and Aslin RN.** Bayesian integration of visual and auditory signals for spatial localization. *J Opt Soc Am A Opt Image Sci Vis* 20: 1391–1397, 2003.
- Becker W and Jurgens R.** An analysis of the saccadic system by means of double step stimuli. *Vision Res* 19: 967–983, 1979.
- Blakemore SJ, Goodbody SJ, and Wolpert DM.** Predicting the consequences of our own actions: the role of sensorimotor context estimation. *J Neurosci* 18: 7511–7518, 1998.
- Bloomberg J, Jones GM, Segal B, McFarlane S, and Soul J.** Vestibular-contingent voluntary saccades based on cognitive estimates of remembered vestibular information. *Adv Otorhinolaryngol* 41: 71–75, 1988.
- Bridgeman B.** A review of the role of efference copy in sensory and oculomotor control systems. *Ann Biomed Eng* 23: 409–422, 1995.
- Buneo CA, Jarvis MR, Batista AP, and Andersen RA.** Direct visuomotor transformations for reaching. *Nature* 416: 632–636, 2002.
- Colby CL, Duhamel JR, and Goldberg ME.** Oculocentric spatial representation in parietal cortex. *Cereb Cortex* 5: 470–481, 1995.
- Colby CL and Goldberg ME.** Space and attention in parietal cortex. *Annu Rev Neurosci* 22: 319–349, 1999.
- Cordo P, Gurfinkel VS, Bevan L, and Kerr GK.** Proprioceptive consequences of tendon vibration during movement. *J Neurophysiol* 74: 1675–1688, 1995.
- Crawford JD and Guitton D.** Visual-motor transformations required for accurate and kinematically correct saccades. *J Neurophysiol* 78: 1447–1467, 1997.
- Crawford JD and Vilis T.** Symmetry of oculomotor burst neuron coordinates about Listing's plane. *J Neurophysiol* 68: 432–448, 1992.
- DeSouza JF, Dukelow SP, Gati JS, Menon RS, Andersen RA, and Vilis T.** Eye position signal modulates a human parietal pointing region during memory-guided movements. *J Neurosci* 20: 5835–5840, 2000.
- Deubel H, Bridgeman B, and Schneider WX.** Immediate post-saccadic information mediates space constancy. *Vision Res* 38: 3147–3159, 1998.
- Dickinson AR, Calton JL, and Snyder LH.** Nonspatial saccade-specific activation in area LIP of monkey parietal cortex. *J Neurophysiol* 90: 2460–2464, 2003.
- Duda RO, Hart PE, and Stork DG.** *Pattern Classification*, (2nd ed.). New York: John Wiley, 2001, p. 680.
- Duhamel JR, Colby CL, and Goldberg ME.** The updating of the representation of visual space in parietal cortex by intended eye movements. *Science* 255: 90–92, 1992.
- Ernst MO and Banks MS.** Humans integrate visual and haptic information in a statistically optimal fashion. *Nature* 415: 429–433, 2002.
- Flanagan JR and Johansson RS.** Action plans used in action observation. *Nature* 424: 769–771, 2003.
- Flanagan JR and Lolley S.** The inertial anisotropy of the arm is accurately predicted during movement planning. *J Neurosci* 21: 1361–1369, 2001.
- Gordon J, Ghilardi MF, Cooper SE, and Ghez C.** Accuracy of planar reaching movements. *Exp Brain Res* 99: 112–130, 1994.
- Gottlieb JP, Kusunoki M, and Goldberg ME.** The representation of visual salience in monkey parietal cortex. *Nature* 391: 481–484, 1998.
- Graf W.** Spatial coordination of compensatory eye movements in vertebrates: form and function. *Acta Biol Hung* 39: 279–290, 1988.
- Graf W and Wilson VJ.** Afferents and efferents of the vestibular nuclei: the necessity of context-specific interpretation. *Prog Brain Res* 80: 149–157, 1989.
- Groh JM and Sparks DL.** Saccades to somatosensory targets. I. Behavioral characteristics. *J Neurophysiol* 75: 412–427, 1996.
- Grill SE and Hallett M.** Velocity sensitivity of human muscle spindle afferents and slowly adapting type II cutaneous mechanoreceptors. *J Physiol* 489: 593–602, 1995.
- Haggard P, Newman C, Blundell J, and Andrew H.** The perceived position of the hand in space. *Percept Psychophys* 62: 363–377, 2000.
- Hallett PE and Lightstone AD.** Saccadic eye movements towards stimuli triggered by prior saccades. *Vision Res* 16: 99–106, 1976.
- Heide W, Binkofski F, Seitz RJ, Posse S, Nitschke MF, Freund HJ, and Kompf D.** Activation of frontoparietal cortices during memorized triple-step sequences of saccadic eye movements: an fMRI study. *Eur J Neurosci* 13: 1177–1189, 2001.
- Helmholtz HV.** *Helmholtz's Treatise on Physiological Optics*. New York: Dover Press, 1962.
- Helsen WF, Elliott D, Starkes JL, and Ricker KL.** Coupling of eye, finger, elbow, and shoulder movements during manual aiming. *J Motor Behav* 32: 241–248, 2000.
- Henriques DY and Crawford JD.** Testing the three-dimensional reference frame transformation for express and memory-guided saccades. *Neurocomputing* 38–40: 1267–1280, 2001.
- Henriques DY, Klier EM, Smith MA, Lowy D, and Crawford JD.** Gaze-centered remapping of remembered visual space in an open-loop pointing task. *J Neurosci* 18: 1583–1594, 1998.
- Henriques DY and Soechting JF.** Bias and sensitivity in the haptic perception of geometry. *Exp Brain Res* 150: 95–108, 2003.
- Henriques DY and Soechting JF.** Haptic synthesis of shapes and sequences. *J Neurophysiol* 91: 1808–1821, 2004.
- Hogan N.** The mechanics of multi-joint posture and movement control. *Biol Cybern* 52: 315–331, 1985.
- Israel I and Berthoz A.** Contribution of the otoliths to the calculation of linear displacement. *J Neurophysiol* 62: 247–263, 1989.
- Jacobs RA.** Optimal integration of texture and motion cues to depth. *Vision Res* 39: 3621–3629, 1999.
- Johansson RS, Westling G, Backstrom A, and Flanagan JR.** Eye-hand coordination in object manipulation. *J Neurosci* 21: 6917–6932, 2001.
- Khan AZ, Pisella L, Rossetti Y, Vighetto A, and Crawford JD.** Impairment of gaze-centered updating of reach targets in bilateral parietal-occipital damaged patients. *Cereb Cortex* 15: 1547–1560, 2005.
- Klier EM and Crawford JD.** Human oculomotor system accounts for 3-D eye orientation in the visual-motor transformation for saccades. *J Neurophysiol* 80: 2274–2294, 1998.
- Lazzari S, Vercher JL, and Buizza A.** Manuo-ocular coordination in target tracking. I. A model simulating human performance. *Biol Cybern* 77: 257–266, 1997.
- Leube DT, Knoblich G, Erb M, Grodd W, Bartels M, and Kircher TT.** The neural correlates of perceiving one's own movements. *Neuroimage* 20: 2084–2090, 2003.
- Lewis RF, Gaymard BM, and Tamargo RJ.** Efference copy provides the eye position information required for visually guided reaching. *J Neurophysiol* 80: 1605–1608, 1998.
- Lynch JC and Tian JR.** Cortico-cortical networks and cortico-subcortical loops for the higher control of eye movements. *Prog Brain Res* 151: 461–501, 2005.
- Maurer C, Kimmig H, Trefzer A, and Mergner T.** Visual object localization through vestibular and neck inputs. I. Localization with respect to space and relative to the head and trunk mid-sagittal planes. *J Vestib Res* 7: 119–135, 1997.
- Mays LE and Sparks DL.** Saccades are spatially, not retinocentrically, coded. *Science* 208: 1163–1165, 1980.
- Medendorp WP, Goltz HC, Vilis T, and Crawford JD.** Gaze-centered updating of visual space in human parietal cortex. *J Neurosci* 23: 6209–6214, 2003.
- Mergner T, Nasios G, and Anastasopoulos D.** Vestibular memory-contingent saccades involve somatosensory input from the body support. *Neuroreport* 9: 1469–1473, 1998.

- Mergner T, Rottler G, Kimmig H, and Becker W.** Role of vestibular and neck inputs for the perception of object motion in space. *Exp Brain Res* 89: 655–668, 1992.
- Messier J and Kalaska JF.** Differential effect of task conditions on errors of direction and extent of reaching movements. *Exp Brain Res* 115: 469–478, 1997.
- Murphy JT, Wong YC, and Kwan HC.** Afferent-efferent linkages in motor cortex for single forelimb muscles. *J Neurophysiol* 38: 990–1014, 1975.
- Mussa-Ivaldi FA, Hogan N, and Bizzi E.** Neural, mechanical, and geometric factors subserving arm posture in humans. *J Neurosci* 5: 2732–2743, 1985.
- Nakamura K and Colby CL.** Updating of the visual representation in monkey striate and extrastriate cortex during saccades. *Proc Natl Acad Sci USA* 99: 4026–4031, 2002.
- Nanayakkara T and Shadmehr R.** Saccade adaptation in response to altered arm dynamics. *J Neurophysiol* 90: 4016–4021, 2003.
- Neggess SF and Bekkering H.** Integration of visual and somatosensory target information in goal-directed eye and arm movements. *Exp Brain Res* 125: 97–107, 1999.
- Neggess SF and Bekkering H.** Ocular gaze is anchored to the target of an ongoing pointing movement. *J Neurophysiol* 83: 639–651, 2000.
- Neggess SF and Bekkering H.** Gaze anchoring to a pointing target is present during the entire pointing movement and is driven by a non-visual signal. *J Neurophysiol* 86: 961–970, 2001.
- Nelson RJ.** Interactions between motor commands and somatic perception in sensorimotor cortex. *Curr Opin Neurobiol* 6: 801–810, 1996.
- Niemeier M, Crawford JD, and Tweed DB.** Optimal transsaccadic integration explains distorted spatial perception. *Nature* 422: 76–80, 2003.
- Pelisson D, Guitton D, and Munoz DP.** Compensatory eye and head movements generated by the cat following stimulation-induced perturbations in gaze position. *Exp Brain Res* 78: 654–658, 1989.
- Plooy A, Tresilian JR, Mon-Williams M, and Wann JP.** The contribution of vision and proprioception to judgements of finger proximity. *Exp Brain Res* 118: 415–420, 1998.
- Pouget A, Ducom JC, Torri J, and Bavelier D.** Multisensory spatial representations in eye-centered coordinates for reaching. *Cognition* 83: B1–B11, 2002.
- Pozzo T, Levik Y, and Berthoz A.** Head and trunk movements in the frontal plane during complex dynamic equilibrium tasks in humans. *Exp Brain Res* 106: 327–338, 1995.
- Sabes PN, Jordan MI, and Wolpert DM.** The role of inertial sensitivity in motor planning. *J Neurosci* 18: 5948–5957, 1998.
- Scheidt RA, Conditt MA, Secco EL, and Mussa-Ivaldi FA.** Interaction of visual and proprioceptive feedback during adaptation of human reaching movements. *J Neurophysiol* 93: 3200–3213, 2005.
- Scherberger H, Cabungcal JH, Hepp K, Suzuki Y, Straumann D, and Henn V.** Ocular counterroll modulates the preferred direction of saccade-related pontine burst neurons in the monkey. *J Neurophysiol* 86: 935–949, 2001.
- Scott SH, Sergio LE, and Kalaska JF.** Reaching movements with similar hand paths but different arm orientations. II. Activity of individual cells in dorsal premotor cortex and parietal area 5. *J Neurophysiol* 78: 2413–2426, 1997.
- Sergio LE, Hamel-Paquet C, and Kalaska JF.** Motor cortex neural correlates of output kinematics and kinetics during isometric-force and arm-reaching tasks. *J Neurophysiol* 94: 2353–2378, 2005.
- Shadmehr R.** Generalization as a behavioral window to the neural mechanisms of learning internal models. *Hum Mov Sci* 23: 543–568, 2004.
- Snyder LH, Batista AP, and Andersen RA.** Coding of intention in the posterior parietal cortex. *Nature* 386: 167–170, 1997.
- Snyder LH, Calton JL, Dickinson AR, and Lawrence BM.** Eye-hand coordination: saccades are faster when accompanied by a coordinated arm movement. *J Neurophysiol* 87: 2279–2286, 2002.
- Sober SJ and Sabes PN.** Multisensory integration during motor planning. *J Neurosci* 23: 6982–6992, 2003.
- Soechting JF, Buneo CA, Herrmann U, and Flanders M.** Moving effortlessly in three dimensions: does Donders' law apply to arm movement? *J Neurosci* 15: 6271–6280, 1995.
- Stahl JS and Simpson JI.** Dynamics of rabbit vestibular nucleus neurons and the influence of the flocculus. *J Neurophysiol* 73: 1396–1413, 1995.
- Stark L and Bridgeman B.** Role of corollary discharge in space constancy. *Percept Psychophys* 34: 371–380, 1983.
- Suzuki Y, Straumann D, Simpson JI, Hepp K, Hess BJ, and Henn V.** Three-dimensional extraocular motoneuron innervation in the rhesus monkey. I. Muscle rotation axes and on-directions during fixation. *Exp Brain Res* 126: 187–199, 1999.
- Tweed D, Cadera W, and Vilis T.** Computing three-dimensional eye position quaternions and eye velocity from search coil signals. *Vision Res* 30: 97–110, 1990.
- Umeno MM and Goldberg ME.** Spatial processing in the monkey frontal eye field. I. Predictive visual responses. *J Neurophysiol* 78: 1373–1383, 1997.
- Van Beers RJ, Baraduc P, and Wolpert DM.** Role of uncertainty in sensorimotor control. *Philos Trans R Soc Lond B Biol Sci* 357: 1137–1145, 2002a.
- Van Beers RJ, Sittig AC, and Denier van der Gon JJ.** How humans combine simultaneous proprioceptive and visual position information. *Exp Brain Res* 111: 253–261, 1996.
- Van Beers RJ, Sittig AC, and Denier van der Gon JJ.** The precision of proprioceptive position sense. *Exp Brain Res* 122: 367–377, 1998.
- Van Beers RJ, Sittig AC, and Gon JJ.** Integration of proprioceptive and visual position-information: an experimentally supported model. *J Neurophysiol* 81: 1355–1364, 1999.
- Van Beers RJ, Wolpert DM, and Haggard P.** When feeling is more important than seeing in sensorimotor adaptation. *Curr Biol* 12: 834–837, 2002b.
- Van Donkelaar P, Siu KC, and Walterschied J.** Saccadic output is influenced by limb kinetics during eye-hand coordination. *J Mot Behav* 36: 245–252, 2004.
- Van Opstal AJ, Hepp K, Hess BJ, Straumann D, and Henn V.** Two- rather than three-dimensional representation of saccades in monkey superior colliculus. *Science* 252: 1313–1315, 1991.
- Vercher JL, Sares F, Blouin J, Bourdin C, and Gauthier G.** Role of sensory information in updating internal models of the effector during arm tracking. *Prog Brain Res* 142: 203–222, 2003.
- Vindras P, Desmurget M, and Viviani P.** Error parsing in visuomotor pointing reveals independent processing of amplitude and direction. *J Neurophysiol* 94: 1212–1224, 2005.
- Walker MF, Fitzgibbon EJ, and Goldberg ME.** Neurons in the monkey superior colliculus predict the visual result of impending saccadic eye movements. *J Neurophysiol* 73: 1988–2003, 1995.
- Welch RB.** *Perceptual Modification*. New York: Academic Press, 1978.
- Welch RB and Warren DH.** Intersensory interactions. In: *Handbook of Perception and Human Performance*, edited by Boff KR, Kaufman L, and Thomas JP. New York: Wiley, 1986, vol. 1, p. 25.
- Welch RB, Widawski MH, Harrington J, and Warren DH.** An examination of the relationship between visual capture and prism adaptation. *Percept Psychophys* 25: 126–132, 1979.
- White JM, Sparks DL, and Stanford TR.** Saccades to remembered target locations: an analysis of systematic and variable errors. *Vision Res* 34: 79–92, 1994.
- Zalkind VI.** Spontaneous discharges of muscle receptors of different functional types. *Fiziol Zh Im I M Sechenova* 65: 565–574, 1979.